View metadata, citation and similar papers at core.ac.uk

brought to you by CORE

provided by Queen Mary Research Online

Structural insights into the loss of catalytic competence in pectate lyase activity at low pH.

Ali, S; Søndergaard, CR; Teixeira, S; Pickersgill, RW

© <2015>. This manuscript version is made available under the CC-BY-NC-ND 4.0 license
http://creativecommons.org/licenses/by-nc-nd/4.0/

For additional information about this publication click this link.
http://qmro.qmul.ac.uk/xmlui/handle/123456789/9970

Information about this research object was correct at the time of download; we occasionally make corrections to records, please therefore check the published record when citing. For more information contact scholarlycommunications@qmul.ac.uk

Structural insights into the loss of catalytic competence in pectate lyase activity at low pH

Salyha Ali[1,2], Chresten R. Søndergaard[3], Susana Teixeira[1,4] & Richard W. Pickersgill[2]

[1] Institut Laue Langevin, 71 Avenue des Martyrs, 38042 Grenoble cedex 9, France.

[2]School of Biological and Chemical Sciences,

Queen Mary University of London, Department of Chemistry & Biochemistry, Mile End Road, London E1 4NS, United Kingdom,

[3]Department of Chemistry, University of Copenhagen, 2100 Copenhagen Denmark

[4]EPSAM, Keele University, Staffordshire ST5 5BG, UK.

To whom correspondence should be addressed: Richard W. Pickersgill, School of Biological and Chemical Sciences, Queen Mary University of London, Mile End Road, London E1 4NS, UK. Tel: +44(0)2078828444; Fax: +44 20 8983 0973; E-mail: r.w.pickersgill@qmul.ac.uk

Highlights

- Two catalytic calcium-ions facilitate proton abstraction in pectate lyase
- At low pH aspartates become protonated and the catalytic calcium-ions are not bound
- The Michaelis complex is not formed in the absence of the catalytic calcium-ions

Abstract

Pectate lyase, a family 1 polysaccharide lyase, catalyses cleavage of the α-1,4 linkage of the polysaccharide homogalacturonan via an *anti* β-elimination reaction. In the Michaelis complex two calcium ions bind between the C6 carboxylate of the *D*-galacturonate residue and enzyme aspartates at the active centre (+1 subsite), they withdraw electrons acidifying the C5 proton facilitating its abstraction by the catalytic arginine. Here we show that activity is lost at low pH because protonation of aspartates results in the loss of the two catalytic calcium-ions causing a profound failure to correctly organise the Michaelis complex.

Keywords

Pectate lyase; pH dependence of activity; Michaelis complex; loss of calcium-binding; catalysis

1. Introduction

Pectate lyases are carbon-oxygen lyases that harness *anti*-β-elimination chemistry to cleave the α-1,4 glycosidic linkage between *D*-galacturonate (GalA) residues in the homogalacturonan region of the plant polysaccharide pectin [1]. In the reaction scheme below R and R' are additional α -1,4 linked GalA residues.

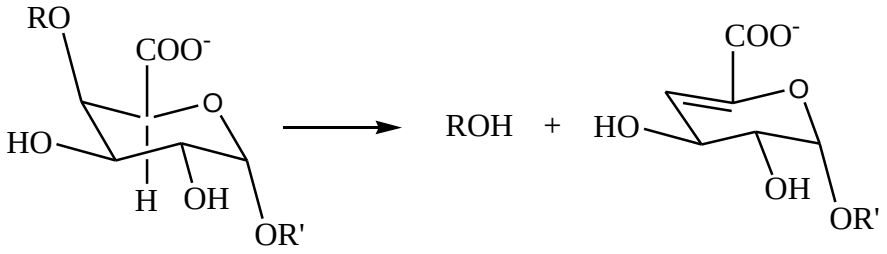

Pectate lyases play a pivotal role in remodelling and recycling the pectin polysaccharides present as insoluble composites in plant cell walls, accelerating rates of reaction by factors exceeding 10^{17} fold and cleaving one of the most stable bonds in nature [2]. Pectate lyases (EC 4.2.2.2) are employed in a range of biotechnological applications involving the extraction and modification of plant polysaccharides and occur in five (PL1, PL3, PL5, PL9 and PL10) of the current 23 families of polysaccharide lyases [3]. *Bacillus subtilis* pectate, the subject of this paper, belongs to PL1 and adopts the parallel β-helix fold [4, 5]. PL3 [6] and PL9 [7] pectate lyases also have this protein architecture as do the fungal pectin lyases A and B [8, 9], rhamnogalacturonase (GH28) [10], polygalacturonase (GH28) [11], and pectin methylesterase (CE8) [12-15]. Pectate lyases in families, PL2 and PL10 enzymes form $(\alpha, \alpha)_7$ and $(\alpha, \alpha)_3$ barrels, respectively [16, 17].

Important insights into the reaction mechanism of PL1 pectate lyase came from complexes formed in PL1 family enzymes [18, 19] and from the discovery of active site convergence in the PL10 and PL1 polysaccharide lyase structures [17]. Several *Bacillus subtilis* pectate lyase substrate complexes in PL1 enzymes have also been reported [20] giving further insights into specificity. A catalytic mechanism featuring acidification of the C5 proton by calcium-ions, proton abstraction from C5 of the GalA residue

binding the +1 subsite with the elimination of the leaving group from C4 is now generally accepted (Fig. 1 & 2; see also the CAZypedia entry on PL1 family polysacharride lyases). Arginine 279 is the catalytic base in pectate lyase which is unusual, but arginine has also been reported to act as the base in other enzymes [21]. *Bacillus subtilis* pectate lyase has a pH optimum of around 8.4 with the activity falling away at low and high pH values [22]. At pH 8.5 the K_M and k_{cat} for trigalacturonate are 1.2 mM and 340 s^{-1}, respectively [20]. Understanding the pH-dependence of this family of enzymes is important for their use in biocatalysis and biotechnology and for engineering enzymes to extend the range of their use for the sustainable utilization of plant polysaccharides. Here, we have studied *B. subtilis* pectate lyase at low pH to understand what changes in structure and electrostatics are responsible for the loss of activity. We discover that loss of activity is due to non-productive binding of substrate caused by protonation of carboxylates that orchestrate formation of the productive Michaelis complex.

2. Materials and Methods

2.1 Production and assay of native pectate lyase

Recombinant *B. subtilis* pectate lyase was produced in *E. coli* as previously described [20]. The activity of the enzyme at different pH values was evaluated by measuring double bond formation in the product at 235nm [22].

2.2 Crystallography

Crystals of *Bacillus subtilis* pectate lyase were grown using hanging drop vapour equilibration using 20 mg/ml protein in 20 mM tris(hydroxymethyl)aminomethane (Tris) at pH 7.0 and a reservoir of 19% (w/v) PEG4000, 0.1 M sodium acetate pH 4.0 and 0.2 M ammonium acetate. The drops were formed using 2µl of each of protein and reservoir. The trigalacturonate complex was produced by soaking crystals in the reservoir conditions supplemented with 5 mM trigalacturonate (Sigma), 2 mM calcium chloride, and 15% glycerol as cryoprotectant for 1 minute prior to cryocooling at 100 K and data collection. These conditions

used are similar to those used previously for the preparation of complexes in crystals of the Arg279Ala mutant previously reported [20], thought the soak time was shorter and the pH lower. The pH in the protein drop is anticipated to be close to pH 4.0 as the Tris buffer is both close to its buffering limit and overwhelmed by the concentration of the acetate buffer. The solubility of the trisaccharide and calcium chloride do not change significantly in going from pH 4.6 to 4.0. Diffraction data were recorded at the European Synchrotron Radiation Facility (ESRF) on the beam-line ID14-1 using the fixed wavelength of 0.934Å, an ADSC Q210 CCD detector and the Oxford Cryostream for 100K data collection. A total of 200 images were collected using 3 second exposures and oscillation of 1° per image up to a resolution of 1.57Å. The crystallographic data statistics are summarized in Table 1. Data were processed and reduced using iMOSFLM [23, 24] and AIMLESS [25, 26], solved using MOLREP [27], and refined and visualized using REFMAC5/ARP [28, 29] and COOT [30], respectively. Calculated anomalous difference maps allowed the calcium-ion to be assigned unambiguously. The refined coordinates and observed structure factor amplitudes are deposited in the protein databank with PDB accession code 5AMV.

2.3 Electrostatic calculations

PROPKA3.1 [31, 32] which can handle multiple ligands and has improved ability to account for non-covalently coupled ionisable groups was used to calculate the *pKa* values for residues in the active centre of the productive and non-productive complexes. The use of PROPKA3.1 allowed three calcium-ions, and trigalacturonate to be included in the calculation using the Michaelis complex and one calcium ion and trigalacturonate in the non-productive complex. The calculations were made at pH 7.0 and pH 4.0 using an intrinsic pKa for the trigalacturonate carboxylates of 3.5 [33].

3. **Results**

Crystals of *B. subtilis* pectate lyase were successfully grown at pH 4.0, soaked in trigalacturonate, calcium and glycerol (cryoprotectant) prior to data collection to 1.57Å resolution (Table 1 gives the crystallographic

statistics). The crystals, of space group $P2_1$ with a=50.8 Å, b=88.1 Å, c=55.5 Å, β=110.4° have a single molecule in the asymmetric unit. The crystal structure, solved by molecular replacement using the native structure (PDB accession code 1BN8) stripped of water molecules and calcium-ion as the search model, showed clear evidence of the binding of trigalacturonate to subsites +2, +3 and +4 and of calcium-ion binding to only the first calcium-binding site (Fig. 3a). The binding to these subsites is not a consequence of an occluded active centre in these crystals as the substrate-binding cleft is open to solvent and there is no steric impediment to binding to subsites +1 and -1, or other subsites to the non-reducing side of the cleaved bond (Fig. 3b). This final structure, comprising residues 1 to 399, trigalacturonate, one calcium-ion, one acetate, one glycerol and 570 waters, could be successfully refined to R-factor/R-free of 16.0/19.2 with reasonable stereochemistry (Table 1). Thirty residues could be built with their side-chains in two conformations. The soak time, although short, is clearly sufficient for trigalacturonate to gain access to the active centre as the occupancy in the crystal is close to 1.0. The high electron density in the native map and peak in the anomalous difference map provides clear evidence of the single calcium-ion bound in the complex. This calcium-ion occupies the site seen in the original, free enzyme, structure and is bound to carboxylate oxygen atoms of aspartates 184, 223 and 227 (Fig. 4a), although in the structure reported here the calcium occupancy is lowered from close to 1.0 to close to 0.5. The oxygen-calcium distances are around 2.3-2.4Å, though it is noticeable that Asp223 adopts two conformations in this structure, one where it is in close contact with the bound calcium (2.3 Å) and one where it has retreated slightly, presumably when the calcium is absent. The tightest interaction between trigalacturonate and enzyme is for the GalA residue in the +2 binding site where the guanidinium group of Arg282 makes two hydrogen bonds with the carboxylate of the galacturonate (Fig. 4b). Other hydrogen bonds from the sugar at the +2 subsite are: O2 to Asn178, O3 to Asp173; O4 and the ring oxygen O5 to Arg279. At the +3 subsite the substrate carboxylate makes polar contacts to Arg217 and Gln278 and at the +4 subsite there are no strong polar interactions but the sugar is secured in place by the binding at the other two sites and the proximity to the enzyme's surface.

The electrostatic results for the productive complex suggest a substantial depression of the *pK* of arginine 279 consistent with its role as base in the reaction. A value of *pKa* 3.2 is calculated for Arg279 at pH 4.0 (Table 2). This *pKa* value is much higher, as expected, for the non-productive complex lacking the catalytic calcium-ions. The four key calcium-binding aspartates all show an upwards movement in *pKa* in the non-productive complex. Asp223 shows the largest shift in *pKa* and this is the calcium-binding residue seen to move away from the first calcium-ion in the electron density map. This movement will hamper binding of the second calcium as will its increase in *pKa*. There is a domino effect as a consequence of not binding of the second calcium, as without this the +1 GalA carboxylate is not correctly positioned to bind the third calcium-ion. The increase in the *pKa* of Asp173 will also contribute to the loss of the third calcium. Asp227 and Asp184 protonation will contribute to the reduced binding affinity of the first calcium ion, movement of Asp223 and the chain of events leading to the non-productive complex. Qualitatively similar shifts between the productive and non-productive complex are seen at pH 7.0 and pH 4.0.

4. Discussion

Previous studies on *B. subtilis* pectate lyase have established that Arg279 is in the correct position to abstract the C5 proton from the GalA binding to the +1 subsite and it is plausible that it is deprotonated for a sufficient fraction of the time to be the essential catalytic base [20]. The electrostatic calculations presented here suggest that the *pKa* of Arg279 is substantially reduced from its intrinsic value consistent with this role in catalysis. Originally we thought that the simplest explanation for the loss of pectate lyase activity at low pH was that the arginine became protonated annulling its ability to abstract the C5 proton from the substrate. However, here we show that the primary reason for loss of activity at low pH is because of non-productive binding to the active centre due to the failure to bind the two catalytic calcium-ions between the enzyme and the substrate. The catalytic calcium-ions are therefore responsible both for inductive destabilization of the C5 proton [5, 34, 35] and for productive binding bringing the C5 proton within reach of the catalytic arginine. The failure to bind the calcium-ions can be traced to the protonation of aspartates that form the binding sites for the catalytic calcium-ions. While protonation of the substrate carboxylates

cannot be ruled out, and may be a contributing factor to loss of Michaelis complex formation, there is direct evidence for protonation of the carboxylates binding the first calcium as the occupancy of this calcium is reduced from close to 1.0 at pH 4.6 [20] to approximately 0.5 at pH 4.0. Although there is evidence from electrostatics calculations to suggest that the *pKa* of all the aspartates is increased, Asp223 appears to play a central role as it links directly the binding of the first calcium-ion through the substrate GalA +1 subsite carboxylate to the second calcium-ion and then indirectly via binding and orientation of the GalA +2 subsite to the third calcium-ion. Furthermore it is Asp223 that moves away from the first calcium-ion in the crystal structure providing a direct link between its behaviour and loss of formation of the productive complex.

Author contributions

SA did the experimental work described in this paper supervised by ST. ST did the final refinement and checking and submitted the coordinates to the protein databank. CS made the electrostatic calculations. RWP designed the experiment, wrote the manuscript, and made the Figures.

Acknowledgements

SA is grateful for funding for a studentship from ILL Grenoble. RWP acknowledges support from Queen Mary University of London and funding from BBSRC (BBS/B/07896). We acknowledge the ESRF Grenoble for beam time on ID14-1 for X-ray data collection.

Figure Legends

Figure 1. The proposed mechanism for the cleavage of trigalacturonate catalysed by pectate lyase in which the C5 proton of the galacturonate (GalA) binding to the +1 subsite of the enzyme is acidified by the binding of two catalytic calcium-ions and abstracted by the catalytic arginine, Arg279. Lysine 247 may also be involved in acidifying the C5 proton by providing a proton to the carboxylate of the galacturonate binding to the +1 subsite. Protonation of the glycosidic oxygen is probably by water. The digalacturonate product has an unsaturated C4-C5 bond.

Figure 2. (a) An overview of the parallel β-helix architecture of *Bacillus subtilis* pectate lyase showing the binding of trigalacturonate to the -1, +1 and +2 subsites formed by the surface of parallel β-sheet PB1 and adjacent loops. The "Michaelis complex" was trapped in the enzyme by substituting the catalytic arginine with alanine [20] (PDB accession code: 2O1D). The arginine, built back into the structure in the position seen in the native structure [5] (PDB accession code: 1BN8), is shown in magenta. Calcium-ions are shown as small cyan spheres. (b) Close-up of the active centre revealing the binding of the two catalytic calcium-ions to the GalA carboxylate in subsite +1. The +2 GalA carboxylate is bound by Arg282 and the -1 GalA carboxylate binds to the first calcium-ion. The crystals were grown at pH 4.6 where there is sufficient activity in the native enzyme for the substrate to be turned over at this pH. PyMOL was used to prepare the Figures showing molecular structures.

Figure 3. (a) σ_A-weighted Fourier synthesis for the non-productive trigalacturonate complex at pH 4.0 (blue chicken wire mesh) with refined structure shown as green carbon and red oxygen atoms. The electron density is contoured at 1.5σ. Also shown is the crystal structure of the productive complex in cyan (PDB accession code: 2O1D). The position of the calcium-ion seen in the non-productive complex is shown as the small orange sphere while the three calcium-ions seen in the productive complex are represented by

three small cyan spheres. At pH 4.6 trigalacturonate substrate binds to subsites -1, +1 and +2. At pH 4.0 trigalacturonate substrate binds subsites +2, +3, +4. (b) A cutaway image showing the active centre of pectate lyase in the context of packing in the monoclinic unit cell. This is an arbitrary view chosen to illustrate that the active centre is open to the solvent channels in the crystal and that the packing does not occlude the binding of the trigalacturonate to any of the major subsites in the enzyme, including +1 and -1. Substrate is drawn as sticks, enzyme in cartoon representation, and calcium-ion as cyan sphere.

Figure 4. σA-weighted Fourier synthesis for the non-productive complex at pH 4.0 contoured a 1.5σ. (a) A single calcium-ion binds at pH 4.0 with an occupancy of approximately 0.5, compared to the occupancy of 1.0 seen at pH 4.6. Asp223 can be seen to have two conformations where only one was detectable at pH 4.6. (b) The hydrogen-bonding interaction between the GalA residue binding at the +2 subsite and Arg282 seen in the complex formed at pH 4.0. This interaction is conserved between the structures at pH 4.6 and 4.0.

Table 1: Crystallographic data statistics

Data collection	
Wavelength (Å)	0.934
Resolution limits (Å)	54.23-1.57 (1.66-1.57)
Space group	$P2_1$
Unit cell *a, b, c* (Å) and β (°)	50.78, 88.12, 55.46, 110.41
Mosaicity (°)	0.93
Total number of reflections	227977
Number of unique reflections	58741
Multiplicity	3.9 (3.8)
Completeness (%)	92.3 (85.5)
<I/σ(I)>	13.7 (3.5)
*R*merge (%)	6.9 (35.8)
*R*p.i.m. (%)	3.9 (20)
B factor from Wilson plot (Å²)	12.5
Crystallographic refinement	
R-factor (%)	16.0
R-free (%)	19.2
Number of reflections used overall / R-free	55740 / 2975
Number of atoms refined	3246 protein /37 trigalacturonate / 570 waters / 1 glycerol / 1 acetate
Free correlation coefficient	0.945
Cruickshank's DPI coordinate error	0.081
Cruickshank's DPI based on R-free	0.084
R.M.S.D. Bond lengths (Å)	0.015
R.M.S.D. Bond angles (°)	1.495
Mean B-factor (Å²)	13.8
Ramachandran outliers	0

The parameter values for the range 1.66–1.57 Å are given in parentheses. $\mathbf{R_{merge}} = \Sigma_{hkl} \Sigma_i |I_i - \langle I \rangle| / -\Sigma_{hkl} \Sigma I_i$, where I_i is the intensity of the i^{th} observation, <I> is the mean intensity of the reflection and the summations extend over all unique reflections (hkl) and all equivalents (i), respectively. **Rpim** is a measure of the quality of the data after averaging the multiple measurements and $R_{pim} = \Sigma_{hkl} [n/(n-1)]^{1/2} \Sigma_i |I_i(hkl) - \langle I(hkl) \rangle| / \Sigma_{hkl} \Sigma_i I_i(hkl)$, where n is the multiplicity, other variables as defined for R_{merge}. **R-factor** = $\Sigma_{hkl} |F_o - F_c| / \Sigma_{hkl} F_o$, where F_o and F_c represent the observed and calculated structure factors, respectively. The R-Factor is calculated using 95% of the data included in refinement and R-free the 5% excluded. **Cruickshank's DPI coordinate error** is Cruickshank's diffraction-component precision index (DPI). **R.M.S.D.:** Root mean square deviation of the refined model values from ideal values.

Table 2: Calculated *pKa* values of residues involved in the Michaelis and non-productive complexes

Residue	Role in Michaelis complex	Michaelis complex pH 7.0	Non-productive complex pH 7.0	Michaelis complex pH 4.0	Non-productive complex pH 4.0	Intrinsic pK_a
D173	Binds Ca1 & Ca2	1.70	2.74	2.62	3.56	3.8
D184	Binds Ca1	7.40	5.84	6.01	7.42	3.8
D223	Binds Ca1 & Ca2	-3.76	-0.13	-4.45	-0.18	3.8
D227	Binds Ca1	2.61	4.36	0.28	3.23	3.8
K247	Close to Ca3	5.93	9.75	1.88	8.42	10.5
R279	Catalytic base	7.58	13.59	3.03	11.42	12.5
R282	Substrate binding	12.59	11.25	9.58	9.35	12.5
R284	Substrate binding	11.47	12.21	11.36	12.05	12.5

The Michaelis and non-productive complexes are described in the text and presented in Fig. 3. The structure used for Michaelis complex calculations was that formed using crystals of the R279A mutant (PDB accession code: 2O1D) with the catalytic arginine reinstated in the position seen in the native structure (PDB accession code: 1BN8).

References

1. Collmer, A. and N.T. Keen, *The Role of Pectic Enzymes in Plant Pathogenesis.* Annual Review of Phytopathology, 1986. **24**: p. 383-409.
2. Wolfenden, R. and M.J. Snider, *The depth of chemical time and the power of enzymes as catalysts.* Accounts of chemical research, 2001. **34**: p. 938-945.
3. Lombard, V., et al., *The carbohydrate-active enzymes database (CAZy) in 2013.* Nucleic Acids Research, 2014. **42**(D1): p. D490-D495.
4. Yoder, M.D., T. Keen N, and F. Jurank, *New domain motif: the structure of pectate lyase C, a secreted plant virulence factor.* Science, 1993. **260**: p. 1503-1507.
5. Pickersgill, R.W., et al., *The structure of Bacillus subtilis pectate lyase in complex with calcium.* Nat Struct Biol, 1994. **1**: p. 717-723.
6. Akita, M., et al., *The first structure of pectate lyase belonging to polysaccharide lyase family 3.* Acta Crystallographica Section D-Biological Crystallography, 2001. **57**: p. 1786-1792.
7. Jenkins, J., et al., *The crystal structure of pectate lyase Pel9A from Erwinia chrysanthemi.* J Biol Chem, 2004. **279**: p. 9139-9145.
8. Mayans, O., et al., *Two crystal structures of pectin lyase A from Aspergillus reveal a pH driven conformational change and striking divergence in the substrate-binding clefts of pectin and pectate lyases.* Structure, 1997. **5**(5): p. 677-689.
9. Vitali, J., et al., *The three-dimensional structure of Aspergillus niger pectin lyase B at 1.7-angstrom resolution.* Plant Physiology, 1998. **116**(1): p. 69-80.
10. Petersen, T.N., S. Kauppinen, and S. Larsen, *The crystal structure of rhamnogalacturonase A from Aspergillus aculeatus: A right-handed parallel beta helix.* Structure, 1997. **5**(4): p. 533-544.
11. Pickersgill, R., et al., *Crystal structure of polygalacturonase from Erwinia carotovora ssp. carotovora.* Journal of Biological Chemistry, 1998. **273**(38): p. 24660-24664.
12. Jenkins, J., et al., *Three-dimensional structure of Erwinia chrysanthemi pectin methylesterase reveals a novel esterase active site.* J Mol Biol, 2001. **305**(4): p. 951-60.
13. Johansson, K., et al., *Crystal structure of plant pectin methylesterase.* FEBS Lett, 2002. **514**(2-3): p. 243-9.
14. Fries, M., et al., *Molecular basis of the activity of the phytopathogen pectin methylesterase.* Embo Journal, 2007. **26**(17): p. 3879-3887.
15. Jenkins, J. and R. Pickersgill, *The architecture of parallel beta-helices and related folds.* Progress in Biophysics & Molecular Biology, 2001. **77**(2): p. 111-175.
16. Abbott, D.W. and A.B. Boraston, *A family 2 pectate lyase displays a rare fold and transition metal-assisted beta-elimination.* Journal of Biological Chemistry, 2007. **282**(48): p. 35328-35336.
17. Charnock, S.J., et al., *Convergent evolution sheds light on the anti-beta-elimination mechanism common to family 1 and 10 polysaccharide lyases.* Proceedings of the National Academy of Sciences of the United States of America, 2002. **99**(19): p. 12067-12072.
18. Scavetta, R.D., et al., *Structure of a plant cell wall fragment complexed to pectate lyase C.* Plant Cell, 1999. **11**(6): p. 1081-1092.
19. Herron, S.R., et al., *Structure and function of pectic enzymes: Virulence factors of plant pathogens.* Proceedings of the National Academy of Sciences of the United States of America, 2000. **97**(16): p. 8762-8769.
20. Seyedarabi, A., et al., *Structural Insights into Substrate Specificity and the anti beta-Elimination Mechanism of Pectate Lyase.* Biochemistry, 2010. **49**(3): p. 539-546.
21. Schlippe, Y.V.G. and L. Hedstrom, *A twisted base? The role of arginine in enzyme-catalyzed proton abstractions.* Archives of Biochemistry and Biophysics, 2005. **433**(1): p. 266-278.

22. Nasser, W., F. Chalet, and J. Robertbaudouy, *PURIFICATION AND CHARACTERIZATION OF EXTRACELLULAR PECTATE LYASE FROM BACILLUS-SUBTILIS.* Biochimie, 1990. **72**(9): p. 689-695.
23. Leslie, A.G., *Integration of macromolecular diffraction data.* Acta Crystallogr D Biol Crystallogr, 1999. **55**: p. 240-255.
24. Battye, T.G.G., et al., *iMOSFLM: a new graphical interface for diffraction-image processing with MOSFLM.* Acta Crystallographica Section D-Biological Crystallography, 2011. **67**: p. 271-281.
25. Evans, P.R. and G.N. Murshudov, *How good are my data and what is the resolution?* Acta Crystallographica Section D-Biological Crystallography, 2013. **69**: p. 1204-1214.
26. Weiss, M.S., *Global indicators of X-ray data quality.* Journal of Applied Crystallography, 2001. **34**: p. 130-135.
27. Vagin, A. and A. Teplyakov, *Molecular replacement with MOLREP.* Acta Crystallographica Section D-Biological Crystallography, 2010. **66**: p. 22-25.
28. Murshudov, G.N., et al., *REFMAC5 for the refinement of macromolecular crystal structures.* Acta Crystallographica Section D-Biological Crystallography, 2011. **67**: p. 355-367.
29. Langer, G., et al., *Automated macromolecular model building for X-ray crystallography using ARP/wARP version 7.* Nature Protocols, 2008. **3**(7): p. 1171-1179.
30. Emsley, P., et al., *Features and development of Coot.* Acta Crystallographica Section D-Biological Crystallography, 2010. **66**: p. 486-501.
31. Sondergaard, C.R., et al., *Improved Treatment of Ligands and Coupling Effects in Empirical Calculation and Rationalization of pK(a) Values.* Journal of Chemical Theory and Computation, 2011. **7**(7): p. 2284-2295.
32. Bas, D.C., D.M. Rogers, and J.H. Jensen, *Very fast prediction and rationalization of pK(a) values for protein-ligand complexes.* Proteins-Structure Function and Bioinformatics, 2008. **73**(3): p. 765-783.
33. Fraeye, I., et al., *Influence of pectin properties and processing conditions on thermal pectin degradation.* Food Chemistry, 2007. **105**(2): p. 555-563.
34. Gerlt, J.A. and P.G. Gassman, *UNDERSTANDING ENZYME-CATALYZED PROTON ABSTRACTION FROM CARBON ACIDS - DETAILS OF STEPWISE MECHANISMS FOR BETA-ELIMINATION REACTIONS.* Journal of the American Chemical Society, 1992. **114**(15): p. 5928-5934.
35. Gerlt, J.A. and P.G. Gassman, *AN EXPLANATION FOR RAPID ENZYME-CATALYZED PROTON ABSTRACTION FROM CARBON ACIDS - IMPORTANCE OF LATE TRANSITION-STATES IN CONCERTED MECHANISMS.* Journal of the American Chemical Society, 1993. **115**(24): p. 11552-11568.

Figure 1

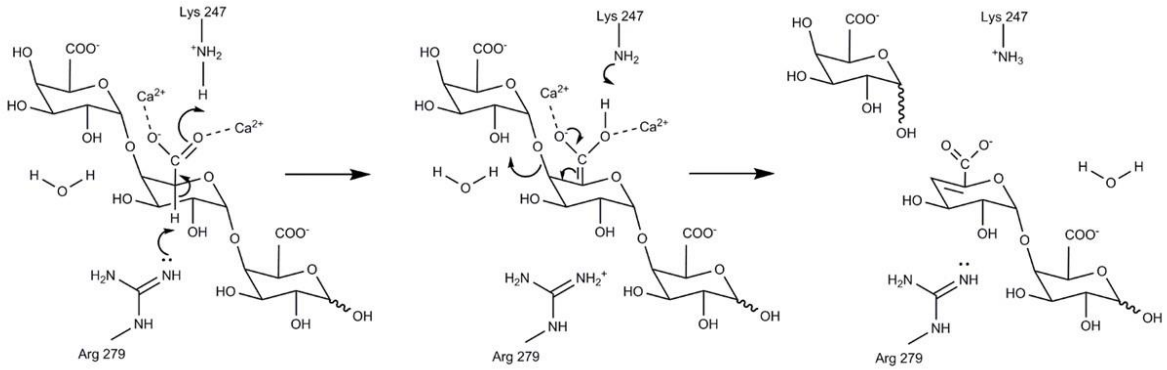

Figure 2

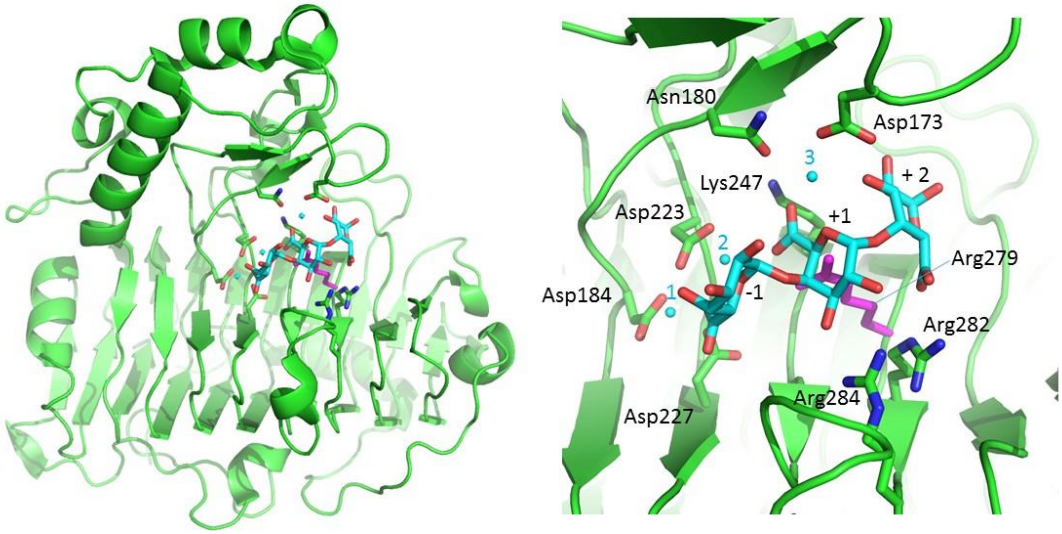
Asn180
Asp173
3
Lys247
+ 2
Asp223
+1
2
Arg279
Asp184
1
-1
Arg282
Arg284
Asp227

Figure 3

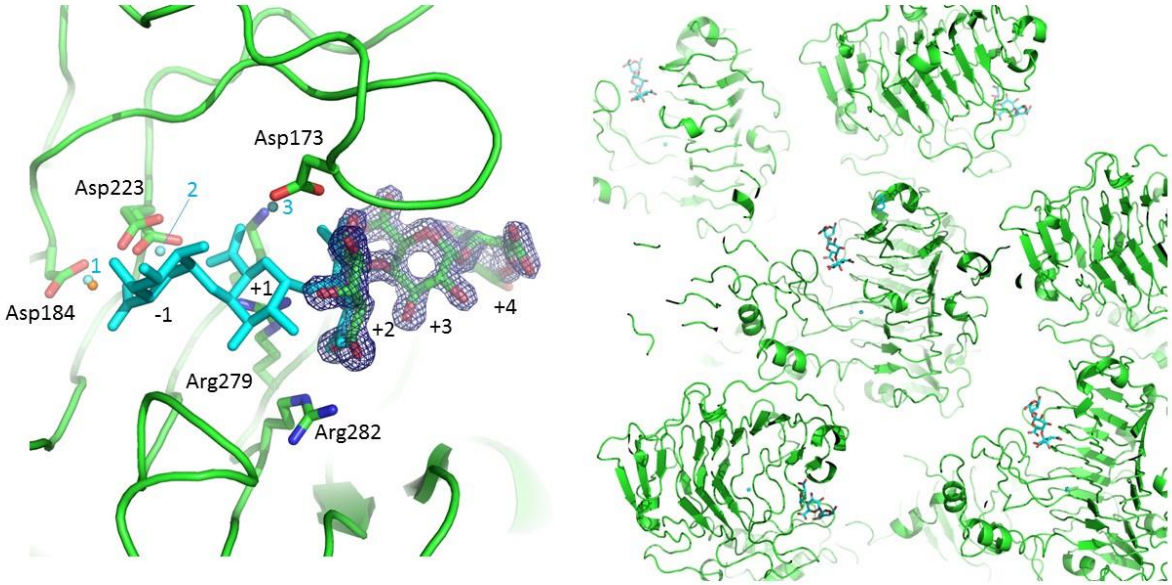

Figure 4